Chronic social stress-induced hyperglycemia in mice couples individual stress susceptibility to impaired spatial memory

Michael A. van der Kooij[a,b,1,2], Tanja Jene[a,b,1], Giulia Treccani[a,b,c], Isabelle Miederer[d], Annika Hasch[a], Nadine Voelxen[e], Stefan Walenta[e], and Marianne B. Müller[a,b]

[a]Translational Psychiatry, Department of Psychiatry, Psychotherapy and Focus Program Translational Neurosciences, University Medical Center, Johannes Gutenberg University Mainz, 55128 Mainz, Germany; [b]German Resilience Center, University Medical Center, Johannes Gutenberg University Mainz, 55128 Mainz, Germany; [c]Translational Neuropsychiatry Unit, Department of Clinical Medicine, Aarhus University, 8000 Aarhus C, Denmark; [d]Department of Nuclear Medicine, University Medical Center, Johannes Gutenberg University Mainz, 55128 Mainz, Germany; and [e]Institute for Pathophysiology, University Medical Center, Johannes Gutenberg University Mainz, 55128 Mainz, Germany

Stringent glucose demands render the brain susceptible to disturbances in the supply of this main source of energy, and chronic stress may constitute such a disruption. However, whether stress-associated cognitive impairments may arise from disturbed glucose regulation remains unclear. Here we show that chronic social defeat (CSD) stress in adult male mice induces hyperglycemia and directly affects spatial memory performance. Stressed mice developed hyperglycemia and impaired glucose metabolism peripherally as well as in the brain (demonstrated by PET and induced metabolic bioluminescence imaging), which was accompanied by hippocampus-related spatial memory impairments. Importantly, the cognitive and metabolic phenotype pertained to a subset of stressed mice and could be linked to early hyperglycemia 2 days post-CSD. Based on this criterion, ~40% of the stressed mice had a high-glucose (glucose >150 mg/dL), stress-susceptible phenotype. The relevance of this biomarker emerges from the effects of the glucose-lowering sodium glucose cotransporter 2 inhibitor empagliflozin, because upon dietary treatment, mice identified as having high glucose demonstrated restored spatial memory and normalized glucose metabolism. Conversely, reducing glucose levels by empagliflozin in mice that did not display stress-induced hyperglycemia (resilient mice) impaired their default-intact spatial memory performance. We conclude that hyperglycemia developing early after chronic stress threatens long-term glucose homeostasis and causes spatial memory dysfunction. Our findings may explain the comorbidity between stress-related and metabolic disorders, such as depression and diabetes, and suggest that cognitive impairments in both types of disorders could originate from excessive cerebral glucose accumulation.

brain | chronic social stress | glucose | metabolism | resilience

The brain consumes about 10 times more calories than the surrounding bodily tissues (1). These substantial cerebral demands for energy, the bulk arriving in the form of glucose from the periphery, may render the brain susceptible to even the slightest disturbances in its energy supply. The impact of psychosocial stress on energy metabolism is increasingly being recognized, and an integrative view may be essential for understanding the mechanisms underlying the adaptation to stress (2, 3). Acute stress constitutes such a disruption: The release of glucocorticoids and norepinephrine during acute stress affects glucose metabolism (4, 5). While a short-lasting, moderate, and controllable stressor is not harmful, and homeostatic recurrence is anticipated, chronic stress may inflict many adverse health effects and has been linked to the emergence of metabolic disorders, including diabetes and cardiovascular disease (6–8). In line with this association, stress-related mental disorders, such as depression, are found to be highly comorbid with diabetes (9). Although disrupted glucose metabolism has been implicated in the pathophysiology of several

brain disorders (10), how long-term chronic stress affects glucose homeostasis and whether these metabolic alterations mediate individual susceptibility or resilience to compromised mental function remain unexplored.

Elements involved in the processing of glucose, including its cerebral uptake (11), have also been implicated in the effects of stress and brain function. Additionally, mitochondria that metabolize glucose were found to shape the stress-related consequences of brain function (12, 13). However, the effects of stress on peripheral and cerebral glucose levels and their consequences for cognitive integrity have largely been neglected. It has been suggested that psychosocial and metabolic stress share common underlying mechanisms with glucose dysregulation having a central role (10, 12, 13). For example, clinical data using PET imaging for cerebral glucose uptake (18F-fluorodeoxyglucose; ^{18}F-FDG) revealed decreased uptake in both depressive disorders and diabetes type 2 (DM2) (14, 15). Interestingly, this decrease was most prominent in DM2 patients that expressed mild cognitive impairments (15), suggesting that DM2-associated mental

Significance

Stress-associated mental disorders and diabetes pose an enormous socio-economic burden. Glucose dysregulation occurs with both psychosocial and metabolic stress. While cognitive impairments are common in metabolic disorders such as diabetes and are accompanied by hyperglycemia, a causal role for glucose has not been established. We show that chronic social defeat (CSD) stress induces lasting peripheral and central hyperglycemia and impaired glucose metabolism in a subgroup of mice. Animals exhibiting hyperglycemia early post-CSD display spatial memory impairments that can be rescued by the antidiabetic empagliflozin. We demonstrate that individual stress vulnerability to glucose homeostasis can be identified early after insult and that stress-induced hyperglycemia directly impinges on cognitive integrity. Our findings further bridge the gap between stress-related pathologies and metabolic disorders.

NEUROSCIENCE

deficits may stem from poor brain glucose metabolism. Additionally, animal models that mimic DM2 and DM2-related metabolic conditions suggest that insulin resistance may be linked to cognitive decline as well, especially in the hippocampus (16). Similarly, insulin resistance also has been associated with the presence of depression (17), and stress-affected hippocampal glucose metabolism is hypothesized to be central in understanding acute stress-induced effects on memory formation (5). The hippocampus is a key brain region involved in spatial memory formation and is a well-recognized target for the effects of chronic stress (18–22). Whether and how a shift in glucose metabolism induced by chronic stress may interfere with learning and memory is still unclear.

Understanding how stress may contribute to metabolic disorders could open up new avenues for treatment and early intervention. In resonance with the appeal to place "gluc" back in glucocorticoids, made a few years ago (12), we investigated the consequences of chronic social stress on glucose metabolism. In a second step, involving stratification of the stressed mice based on individual glucose levels after chronic social defeat (CSD), we explored the reversibility of hyperglycemia-associated spatial memory impairments by treatment with the glucose-lowering antidiabetic compound empagliflozin (EMPA).

Results

CSD Causes Hyperglycemia, Hypercortisolemia, Adrenal Hyperplasia, and Hyperphagia.
The long-term effects of stress on glucose metabolism and their consequences have not been fully elucidated. We first studied the effects of CSD on glucose levels in the peripheral blood. During CSD lasting 10 consecutive days glucose levels initially tended to drop for stressed mice (day 8) but were significantly increased on the morning of day 12 (i.e., 2 d post-CSD) in comparison with timed controls (Fig. 1A). The high glucose levels found in these CSD-exposed animals at 2 d post-CSD were associated with increased corticosterone levels that we detected simultaneously (Fig. 1B). However, the blood plasma levels of corticosterone 2 d post-CSD did not correlate with their glucose levels (*SI Appendix*, Fig. S1A). The lasting impact of our CSD paradigm on stress physiology was further demonstrated by hyperplasia/hypertrophy of the adrenal glands 5 d post-CSD (Fig. 1C). Furthermore, body weight was not affected throughout or after the stressful period, but stressed mice did increase their daily food intake throughout and after the CSD (Fig. 1D and *SI Appendix*, Fig. S1 B and C). However, blood plasma leptin concentrations were not affected by CSD (Fig. 1E).

CSD Perturbs Peripheral Glucose Metabolism and Affects Behavior.
The behavioral impact of a social defeat paradigm can be validated in a confrontation test; stressed mice typically show a reduction in the exploration of an unknown mouse that appears similar to the mouse by which it was defeated during CSD (23). Indeed, CSD-exposed mice displayed reduced exploration of the unknown CD-1 mouse in the confrontation test (Fig. 2 A and B). Following CSD, hyperglycemia develops and lasts for at least 2 wk (Fig. 2C). We investigated the impact of CSD on the expression of stress hormones, on glucose and insulin metabolism, and on behavioral functions during this hyperglycemic phase. One week after CSD, we found that both morning and afternoon circulating corticosterone levels did not differ between control and CSD-exposed mice (*SI Appendix*, Fig. S1D). Glucose metabolism was perturbed for CSD-exposed animals; in a glucose tolerance test (GTT) performed 9 d post-CSD in fasted animals, glucose levels were increased 30 min after a glucose bolus injection compared with control mice (Fig. 2D). In contrast, insulin sensitivity appeared intact in CSD-exposed mice, as blood plasma insulin concentrations did not differ from controls or when insulin levels obtained from animals before the onset of CSD were compared with samples taken 8 d post-CSD (*SI Appendix*, Fig. S1E). Additionally, the glucose response to an insulin bolus in the insulin-tolerance test and the insulin response to a glucose bolus in the GTT did not reveal differences between control and CSD-exposed mice (*SI Appendix*, Fig. S1 F and G). On a behavioral level we found extended immobility in the forced swim test for CSD-exposed animals (Fig. 2E). While basic novel object memory remained intact (Fig. 2F), spatial memory appeared to be specifically impaired, as CSD-exposed mice did not show a preference for the novel arm in a cognitive version of the Y-maze (Fig. 2 G and H). Although CSD-exposed animals displayed a modest reduction (−18.7%) in locomotor activity during the exploration phase in the Y-maze, the amount of locomotor activity did not correlate with Y-maze performance in either CSD-exposed or control mice (*SI Appendix*, Fig. S2). We thus can exclude locomotor activity as a potential confounder of the effects of CSD on cognitive function. The amount of CD-1 exploration of the unknown CD-1 mouse correlated positively with the cognitive deficits in the Y-maze (Fig. 2I), indicating that stress severity may predict spatial memory impairments. The spatial memory impairments displayed by CSD-exposed mice were confirmed in the object location task (Fig. 2J). In the light–dark box we found no differences in time spent in the light compartment, total number of light–dark transitions, or the latency to first entry into the dark compartment (*SI Appendix*, Fig. S3), indicating that the stress-induced spatial memory impairments were not driven by altered anxiety-like behavior. Since glycosylated hemoglobin (HbA1c) was increased when measured 8 wk post-CSD (Fig. 2K), the molecular consequences of hyperglycemia can persist beyond the duration of increased blood glucose levels.

CSD-Induced Cerebral Hyperglycemia Is Linked to Spatial Memory Impairments.
We wondered whether the pervasive effects of CSD on peripheral glucose levels and its metabolism would also affect the brain. Seeing that CSD impaired spatial memory, we were particularly interested in the involvement of the hippocampus, a

Fig. 1. CSD causes hyperglycemia, hypercortisolemia, adrenal hyperplasia, and hyperphagia. (A) Blood glucose levels in stressed mice were increased at 2 d post-CSD [interaction: $F_{(2,90)} = 7.65$, $P < 0.001$, $n = 23$ or 24 per group, comparing days 4–12 (t = 3.12, df = 90, $P < 0.01$) and days 8–12 (t = 3.27, df = 90, $P < 0.01$)]. (B) Morning levels of blood plasma corticosterone were increased in CSD-exposed animals at 2 d post-CSD (t = 2.62, df = 35, $P = 0.013$, $n = 18$ or 19 per group). (C and D) CSD-exposed animals exhibited increased adrenal weight (t = 7.02, df = 18, $P < 0.001$, $n = 10$ per group) (C) and hyperphagia throughout CSD (t = 3.80, df = 10, $P = 0.004$) (D). (E) Blood plasma leptin levels taken 1 wk post-CSD did not differ between CSD-exposed and control (CTRL) mice (t = 0.55, df = 28, $P = 0.59$, $n = 14$–16 per group). Data are presented as mean + SEM; *$P < 0.05$, **$P < 0.01$, ***$P < 0.001$, Student's t test in B–D and two-way repeated-measures ANOVA with Bonferroni's posttest in A.
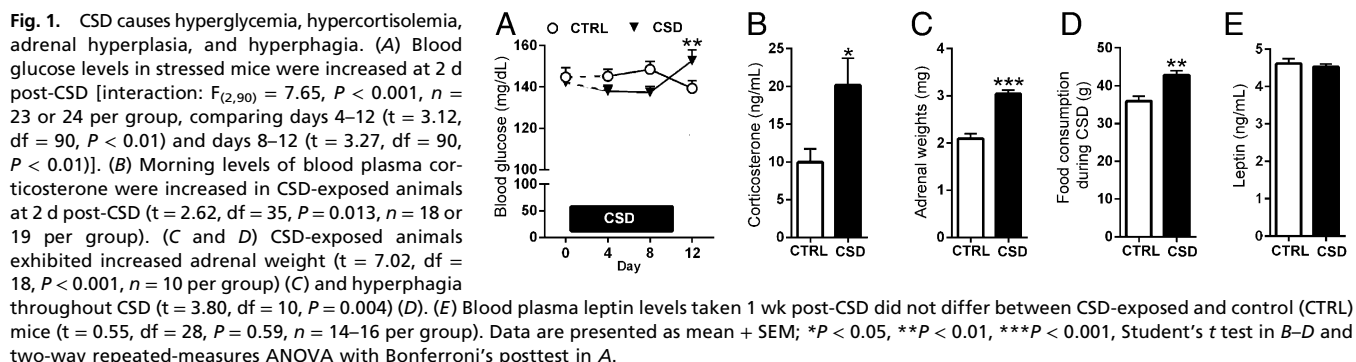
Fig. 2. CSD perturbs glucose metabolism and affects behavior. (*A* and *B*) Control (CTRL) mice readily explore a cylinder containing an unknown CD-1 mouse placed in the center of an open field arena, but CSD-exposed mice show less exploration [depicted by representative heat maps (*A*) and quantified (*B*): t = 2.85, df = 16, *P* = 0.012, n = 9 per group]. (*C*) Peripheral hyperglycemia develops post-CSD and lasts ~2 wk before returning to baseline [time: $F_{(4,72)}$ = 2.81, *P* = 0.032; CSD: $F_{(1,18)}$ = 12.68, *P* = 0.002; interaction: $F_{(4,72)}$ = 8.53, *P* < 0.001, n = 10 per group]. Glucose levels differed at 1 wk (t = 5.44, df = 90, *P* < 0.001) and 2 wk (q = 4.56, df = 90, *P* < 0.001) post-CSD. Behavioral testing (except the CD-1 encounter) and the GTT took place during this hyperglycemic period. Long-term effects of CSD were measured by HbA1c 8 wk post-CSD. (*D*) In the GTT, CSD-exposed mice displayed delayed recovery from a glucose bolus (2 g/kg i.p.) [interaction: $F_{(4,72)}$ = 3.64, *P* = 0.009; time: $F_{(4,72)}$ = 49.91, *P* < 0.001; n = 10 per group with differences at 30 min (t = 4.13, df = 90, *P* < 0.001)]. (*E*) CSD-exposed mice exhibited increased immobility time in the forced swim test compared with control mice (t = 3.17, df = 19, *P* = 0.005, n = 9–12 per group). (*F*) Novel object preference was intact with no CSD effects [performance against chance for control mice (t = 6.28, df = 18, *P* < 0.001) and for CSD-exposed mice (t = 4.15, df = 18, *P* < 0.001); CSD (t = 0.64, df = 36, *P* = 0.52, n = 19 per group)]. (*G* and *H*) Control mice explored the novel (NEW) arm of the Y-maze more than the familiar (FAM) arm, but CSD-exposed mice did not display this preference [depicted by representative heat maps (*G*) and quantified (*H*): against chance for control mice: t = 5.79, df = 9, *P* < 0.001; for CSD-exposed mice: t = 0.06, df = 9, *P* = 0.95;

CSD: t = 2.86, df = 18, *P* = 0.01, n = 10 per group]. (*I*) CD-1 exploration correlated positively with novel arm preference in the Y-maze; the regression line is shown with the 95% confidence interval (dotted lines) (r = 0.67, r^2 = 0.45, *P* = 0.034). (*J*) Control mice displayed a preference for the replaced object in the object location task (t = 5.23, df = 14, *P* < 0.001), but this preference was not seen for CSD-exposed mice (t = 1.62, df = 12, *P* = 0.13). (*K*) HbA1c in the peripheral blood was increased for stressed mice 8 wk post-CSD (t = 3.96, df = 19, *P* < 0.001, n = 10 or 11 per group). Data are presented as mean + SEM; **P* < 0.05, ***P* < 0.01, ****P* < 0.001, Student's t test in *B*, *E*, *F*, *H*, and *J*; one-sample t test against chance in *F* and *H*; Pearson's correlation coefficient in *I*; one-way repeated-measures ANOVA with Bonferroni's posttest in *C*; or two-way repeated-measures ANOVA with Bonferroni's posttest in *D*.
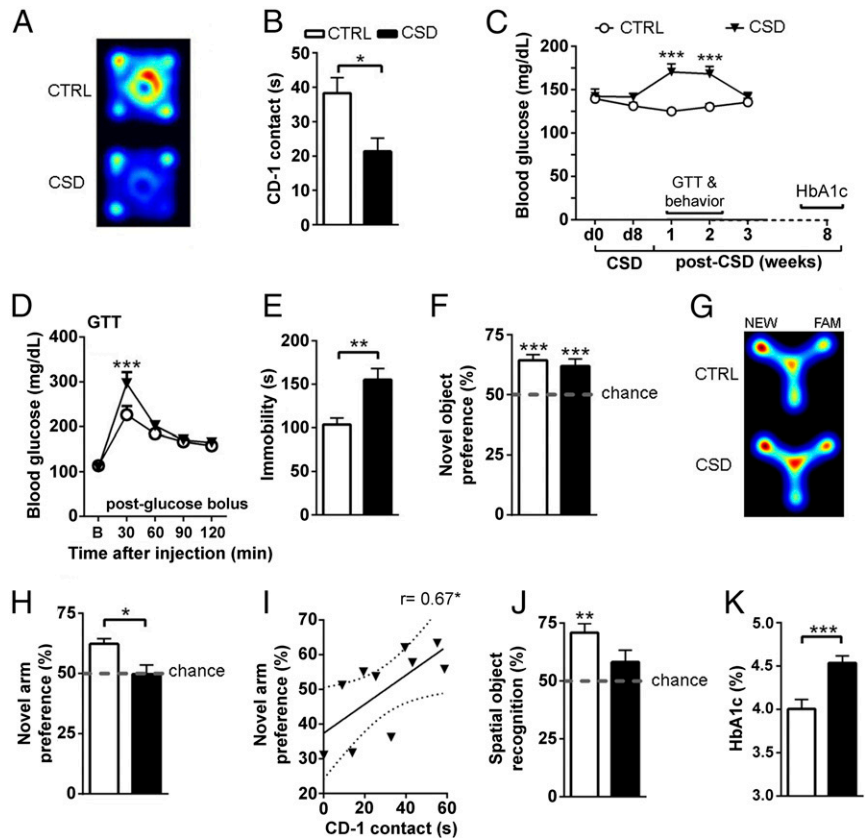
brain region known to be highly sensitive to the effects of chronic stress. Induced metabolic bioluminescence imaging (imBI) of glucose is based on bioluminescence reactions: Tissue glucose is enzymatically linked to the light reaction, resulting in a calibrated, color-coded 2D image of microscopic glucose distribution within a tissue section. ImBI revealed hyperglycemia throughout the stressed brain (Fig. 3*A*). Peripheral glucose levels taken when these animals were killed were predictive of cerebral glucose levels, indicating that cerebral and peripheral hyperglycemia were linked (Fig. 3*B*). The cerebral hyperglycemia pertained to the hippocampal formation as well (Fig. 3 *C* and *D*). Interestingly, animals' hippocampal-dependent Y-maze performance (Fig. 2 *G* and *H*) correlated negatively with the amount of hippocampal glucose found using glucose imBI (Fig. 3*E*), suggesting that the hyperglycemia in the hippocampus may be detrimental to its function. In agreement with this notion, intrahippocampal glucose infusion to nonstressed mice impaired spatial memory in the Y-maze test (Fig. 3 *F* and *G*); the injection sites were verified postmortem, and a representative image is shown in Fig. 3*H*. To investigate putative cellular disturbances induced by hippocampal hyperglycemia, we measured levels of NAD^+, NADH, and malondialdehyde [as an estimation for thiobarbituric acid (TBARS)] during CSD (day 10) and thereafter (3 and 5 wk post-CSD) but found no changes (*SI Appendix*, Table S1).

Cerebral Glucose Uptake Is Reduced in Mice That Underwent CSD. To gain insight into the cerebral metabolism of glucose under stress, we measured cerebral ^{18}F-FDG uptake and found an overall decrease in whole-brain ^{18}F-FDG uptake in CSD-exposed mice

as compared with controls (Fig. 4 *A* and *B*). A follow-up analysis revealed that the stress-induced reduction of ^{18}F-FDG uptake included the hippocampal formation, among other selected regions (Fig. 4*C* and *SI Appendix*, Fig. S4). In line with the decreased ^{18}F-FDG uptake, CSD-exposed animals exhibited a reduction of hippocampal glucose transporter 1 (GluT1) membrane protein levels (Fig. 4*D*). For GluT1, we observed two adjacent bands; due to their proximity, we analyzed them collectively. The masses of these 45- and 55-kDa bands correspond to the two known isoforms of GluT1 and are localized to glial cells and endothelial cells, respectively (24). We detected only one band in the membrane fractions stained for GluT3 and GluT4, and their protein levels were unaltered after stress (Fig. 4 *E* and *F*). Cytosolic hippocampal protein levels for GluT1, GluT3, and GluT4 did not differ between CSD-exposed mice and controls (*SI Appendix*, Table S2).

EMPA Rescues CSD-Induced Disturbances in Glucose Metabolism and Spatial Memory for Stressed Mice Preidentified as Having High Glucose Levels. Spurred by our finding that stress induced hyperphagia during CSD, we explored whether stress-induced hyperglycemia and the associated cognitive impairments could be prevented by caloric restriction. Caloric restriction was imposed during CSD (10 consecutive days) by supplying animals with 80% of their prestress defined ad libitum food intake (*SI Appendix*, Fig. S5*A*). This procedure caused a temporary decrease in the animals' bodyweight (*SI Appendix*, Fig. S5*B*). However, caloric restriction did not prevent the development of the poststress hyperglycemic phenotype, nor did it ameliorate stress-induced
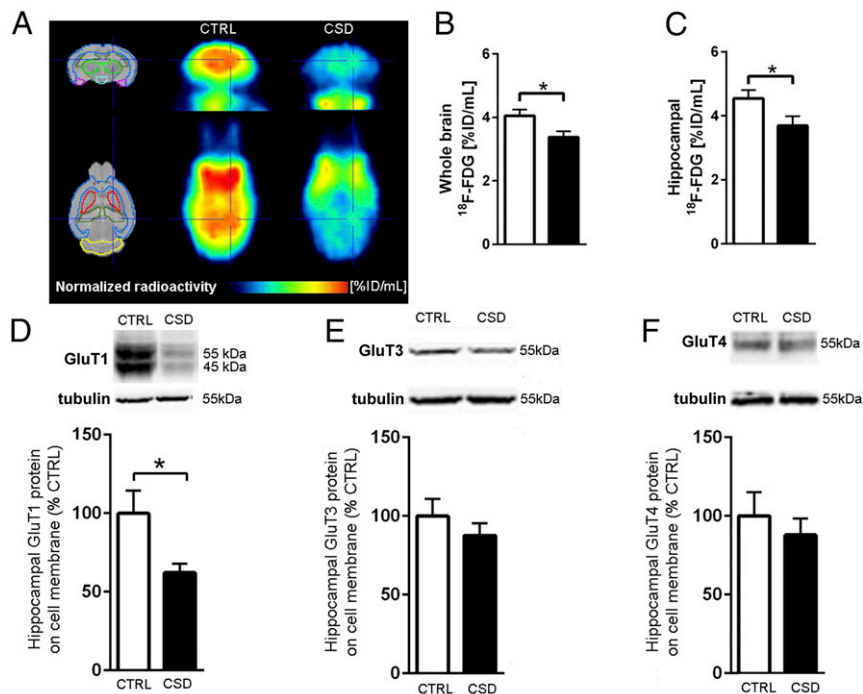
Fig. 3. CSD induces cerebral hyperglycemia. (*A*) Brain glucose levels of CSD-exposed animals were increased compared with controls (CTRL) (t = 2.61, df = 10.47, $P = 0.025$, n = 10 per group). (*B*) Peripheral blood glucose levels correlated positively with cerebral glucose levels (r = 0.52, $r^2 = 0.27$, $P = 0.018$). (*C*) The cerebral hyperglycemia also pertained to the hippocampus. (*Top*) H&E staining. (*Middle* and *Bottom*) Bioluminescent signal for control mice (*Middle*) and CSD-exposed mice (*Bottom*). (*D*) Quantification of hippocampal glucose (t = 2.53, df = 11.58, $P = 0.027$, n = 10 per group; white bar, control; black bar, CSD). (*E*) Hippocampal glucose correlated negatively with spatial memory performance (r = −0.47, $r^2 = 0.22$, $P = 0.037$). (*F*) Glucose/saline was infused into the hippocampus, and mice were tested in the Y-maze. (*G*) Glucose-infused mice did not display a preference in novel arm exploration, unlike vehicle-infused mice (vehicle infusion: t = 3.93, df = 8, $P = 0.004$; glucose infusion: t = 0.40, df = 7, $P = 0.70$), and intrahippocampal glucose reduced novel arm preference compared with vehicle-treated control mice (t = 2.19, df = 15, $P = 0.045$, n = 8 or 9 per group). (*H*) Verification of the hippocampal injection. (*Right*) A representative image of the injection site (in blue). (*Left*) The corresponding Nissl-stained histological plate. Image courtesy of © 2004 Allen Institute for Brain Science. Allen Mouse Brain Atlas. Available from: http://mouse.brain-map.org/experiment/siv?id=100142143&imageId=102162210&imageType=atlas&initImage=atlas&showSubImage=y&contrast=0.5,0.5,0,255,4. Data are presented as mean + SEM; *$P < 0.05$, Student's t test in *A*, *D*, and *G* with Pearson's correlation coefficient in *B* and *E*. Regression lines are shown with the 95% confidence interval (dotted lines) in *B* and *E*.

cognitive impairments in the Y-maze (*SI Appendix*, Fig. S5 *C* and *D*). We then investigated whether a treatment specifically targeting stress-induced hyperglycemia and starting after CSD might normalize stress-induced disturbances in glucose metabolism and improve cognitive integrity. We first studied the effects of the SGLT2 inhibitor EMPA ingested via food in a pilot experiment on control mice. As expected, EMPA treatment (lasting 8 d) significantly reduced peripheral blood glucose levels (Fig. 5*A*). The glucose concentrations of these control EMPA-treated mice varied, and we stratified these mice based on the glucose values expressed by the control vehicle-treated mice (mean ± SD) into those exhibiting low glucose (L-Gluc, <125 mg/dL), intermediate glucose (Int-Gluc, 125–150 mg/dL), or high glucose (H-Gluc, >150 mg/dL) (Fig. 5*B*). Interestingly, the performance of these EMPA-treated animals in the Y-maze could be predicted based on this stratification: Whereas control vehicle-treated animals displayed the anticipated novel arm preference, control L-Gluc EMPA-treated mice did not show a novel arm preference, in contrast with the intact performance of the control Int-Glu EMPA-treated mice (Fig. 5*C*). Thus, both stress-induced high glucose and low peripheral glucose levels can be linked to spatial memory impairments. We next wanted to investigate whether EMPA treatment begun early post-CSD could prevent the stress-

induced disturbances at the level of glucose metabolism and rescue cognitive integrity. However, reanalyzing the first occurrence of stress-induced hyperglycemia 2 d post-CSD (day 12) (Fig. 1*A*) revealed that only 36% of the CSD-exposed animals exhibited high peripheral blood glucose (>150 mg/mL). We therefore were mindful that EMPA could introduce cognitive deficits in those CSD-exposed animals that retained intermediate blood glucose levels by subsequently lowering their glucose levels, a situation similar to the one we observed for control animals treated with low glucose/EMPA (Fig. 5 *B* and *C*). Hence, we set up an experiment that takes into account the possibility that differential CSD-induced effects on the animals' glucose status could determine the impact of EMPA. In a new set of animals we observed again that overall blood glucose levels were increased for CSD-exposed mice at 2 d post-CSD, and we classified these animals into those exhibiting a H-Gluc (>150 mg/dL), Int-Gluc (>125, <150 mg/dL), or L-Gluc (<125 mg/dL) profile (Fig. 5*D*). EMPA treatment commenced immediately after classification and led to detectable glucose in urine 7 d later, regardless of the animals' predefined glucose phenotype (Fig. 5*E*). Consequently, EMPA treatment reduced peripheral blood glucose levels in CSD-exposed mice (*SI Appendix*, Fig. S6). In the Y-maze we found a significant interaction: Spatial memory performance in the Y-maze

Fig. 4. CSD reduced cerebral glucose uptake and decreased hippocampal protein expression of GluT1. (*A*) ^{18}F-FDG uptake in the whole brain was reduced in CSD-exposed mice compared with control mice as shown by PET scans obtained by overlay from the individual PET signals. (*B* and *C*) Results in *A* quantified for the whole brain (t = 2.50, df = 15, P = 0.025, n = 8 or 9 per group) (*B*) and for the hippocampus (t = 2.17, df = 15, P = 0.047, n = 8 or 9 per group) (*C*). (*D–F*) Hippocampal membrane protein levels were reduced for GluT1 (t = 2.45, df = 9.2, P = 0.036) (*D*) but not for GluT3 (t = 0.94, df = 15, P = 0.40) (*E*) or GluT4 (t = 0.66, df = 14, P = 0.52) (*F*). Data are presented as mean + SEM; *P < 0.05, Student's t test in *B–D*.

deteriorated for EMPA-treated CSD mice previously characterized with an In-Gluc phenotype, but EMPA treatment improved the poor Y-maze default performance shown by CSD-exposed mice that were preidentified as having the H-Gluc phenotype (Fig. 5F). In agreement with the hypothesis that CSD-induced hyperglycemia impairs spatial memory but EMPA treatment benefits only the stressed mice that develop hyperglycemia (defined here as >150 mg/dL at 2 d post-CSD), we see that novel arm preference in the Y-maze correlates negatively with the 2-d post-CSD blood glucose levels in vehicle-treated CSD mice (Fig. 5G) but positively with 2-d post-CSD blood glucose values in EMPA-treated CSD animals (Fig. 5H). In contrast, cognitive performance in the Y-maze did not correlate with peripheral glucose levels in control mice (*SI Appendix*, Fig. S7), suggesting that the effects of blood glucose levels on Y-maze performance pertain only to CSD-exposed mice. In line with the behavioral findings, and highlighting the lasting effects of CSD on glucose metabolism, a GTT performed 3 wk post-CSD revealed that only vehicle-treated CSD/H-Gluc mice displayed impaired glucose metabolism, whereas EMPA treatment normalized glucose breakdown in CSD mice exhibiting the H-Gluc phenotype (Fig. 5I). Since exploration in the confrontation test is frequently taken as a proxy for stress susceptibility versus resilience, we correlated these measurements to the blood glucose levels 2 d post-CSD but found no association (*SI Appendix*, Fig. S8).

Discussion

Stress increases the levels of circulating glucose, and chronic stress may lead to the development of physiological as well as cognitive impairments, especially in individuals that lack proper adaptive mechanisms (25). It remains to be determined, however, whether (central) glucose dysregulation is linked to stress-induced cognitive impairments and whether abnormal glucose metabolism may contribute to individual susceptibility to the aversive consequences of chronic stress. Here, we discovered that CSD in male mice lastingly increases peripheral and central glucose levels and affects glucose metabolism and that these perturbations are causally related to the emergence of stress-induced cognitive impairments. Notably, we could rescue this metabolic and cognitive phenotype by the SGLT2 inhibitor EMPA, which lowers glucose concentrations by stimulating renal glucose excretion (26).

Specifically, we show that peripheral and central hyperglycemia ensue in the weeks following CSD but are not present during the stressful period itself. With respect to glucose metabolism, the results from the GTT suggest abnormal glucose breakdown in stressed mice. Since the stressed brain is hyperglycemic but also displays a reduction of cerebral ^{18}F-FDG uptake, as shown here, our findings suggest that the CSD-induced hyperglycemia may not simply be a direct consequence of meeting increased brain glucose demands but also could be dysfunctional and maladaptive for cognition. This possibility is further accentuated with the observed negative correlations between peripheral and central (hippocampal) glucose and spatial memory performance. Moreover, the impaired spatial memory induced by intrahippocampal infusion of glucose (comparable to the hippocampal glucose levels found in CSD-exposed mice) supports the interpretation that stress-induced cerebral hyperglycemia may be sufficient to cause cognitive deficits.

Although all stressed animals in our study were subjected to exactly the same duration of aggressive behavior (30 s/d), only a fraction (36%) of CSD-exposed animals were identified as H-Gluc (glucose levels >150 mg/mL) at 2 d post-CSD, whereas a considerable proportion maintained glucose levels within a normal range (glucose levels <150 mg/mL and >125 mg/mL) at 2 d post-CSD. Other studies involving social defeat have classically segregated subjects into susceptible versus resilient individuals (23, 27), and such a classification was applied to the
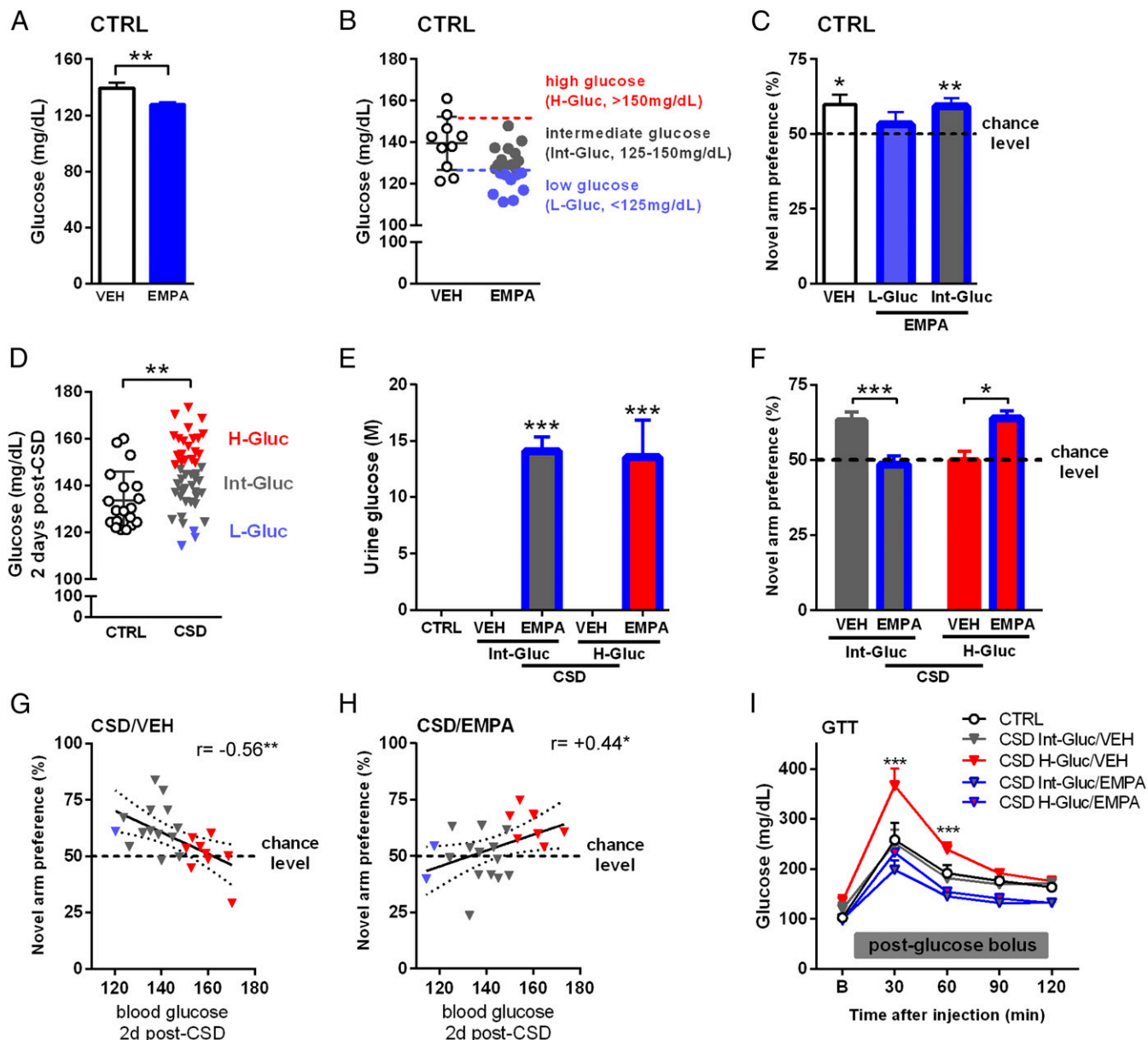
NEUROSCIENCE

Fig. 5. EMPA treatment impedes CSD-induced disturbances in glucose metabolism and rescues spatial memory for H-Gluc mice but is detrimental to Int-Gluc animals. (A) In control animals, EMPA reduced peripheral glucose (t = 3.01, df = 30, P = 0.005; vehicle-treated control mice, n = 10; EMPA-treated control mice, n = 22). (B) EMPA-treated control mice were classified as H-Gluc (>150 mg/dL), Int-Gluc (125–150 mg/dL), or L-Gluc (<125 mg/dL) based on peripheral blood glucose values (mean ± SD) of vehicle-treated control mice. (C) In the Y-maze, vehicle-treated control mice and EMPA-treated control Int-Gluc mice showed intact novel arm preference, whereas EMPA-treated control L-Gluc mice did not reveal a preference (against chance for control vehicle-treated mice: t = 3.03, df = 9, P = 0.014; for EMPA-treated control L-Gluc mice: t = 0.77, df = 8, P = 0.46; and for EMPA-treated control Int-Gluc mice: t = 3.55, df = 12, P = 0.004; n = 9–13 per group). (D) CSD-exposed mice displayed increased blood glucose levels compared with control mice 2 d post-CSD (t = 3.00, df = 64, P = 0.004, n = 19 and 47 per group, respectively) and were classified into H-Gluc, Int-Gluc, and L-Gluc groups. (E) Glucose was detected in the urine of EMPA-treated mice only [treatment: $F_{(1,20)}$ = 59.51, P < 0.001, n = 5–7 per group; Int-Gluc: t = 5.81, df = 20, P < 0.001; H-Gluc: t = 5.14, df = 20, P < 0.001]. (F) In the Y-maze, EMPA treatment worsened the performance of the CSD/Int-Gluc group compared with the vehicle-treated CSD/Int-Gluc group [interaction: $F_{(1,42)}$ = 23.24, P < 0.001, n = 8–15 per group; Int-Gluc: t = 4.08, df = 42, P < 0.001]. In contrast, vehicle-treated CSD/H-Gluc mice did not show a novel arm preference, but EMPA treatment of CSD/H-Gluc mice rescued these spatial memory impairments (H-Gluc: t = 2.95, df = 42, P < 0.05). (G) In vehicle-treated CSD mice Y-maze performance correlated negatively with peripheral glucose levels 2 d post-CSD (r = −0.56, r^2 = 0.31, P = 0.005). (H) In contrast, for EMPA-treated CSD mice, Y-maze performance correlated positively with peripheral glucose levels 2 d post-CSD (r = 0.44, r^2 = 0.19, P = 0.03). (I) In the GTT performed 3 wk post-CSD vehicle-treated CSD/H-Gluc mice showed impaired glucose metabolism, which was normalized for EMPA-treated CSD/H-Gluc mice [interaction: $F_{(12,80)}$ = 3.78, P < 0.001; time: $F_{(4,80)}$ = 85.26; P < 0.001; treatment: $F_{(3,20)}$ = 17.82, P < 0.001; n = 5–9 per group]. For significant effects at 30 min, vehicle-treated CSD/Int-Gluc mice vs. EMPA-treated mice CSD/Int-Gluc: t = 2.91, df = 100, P < 0.05; in vehicle-treated CSD/H-Gluc mice vs. EMPA-treated CSD/H-Gluc mice: t = 6.74, df = 100, P < 0.001; in vehicle-treated CSD/Int-Gluc mice vs. vehicle-treated CSD/H-Gluc mice: t = 5.80, df = 100, P < 0.001; and for significant effects at 60 min, in vehicle-treated CSD/H-Gluc mice vs. EMPA-treated mice CSD/H-Gluc mice: t = 4.27, df = 100, P < 0.001; in vehicle-treated CSD/Int-Gluc mice vs. vehicle-treated mice CSD/H-Gluc mice: t = 2.89, df = 100, P < 0.05. Data are presented as mean ± SEM in A, C, E, F, and I and as mean ± SD in B and D; *P < 0.05, **P < 0.01, ***P < 0.001, Student's t test in A and D, one-sample t test against chance in C and F, two-way ANOVA with Bonferroni's posttest in E, F, and I, or Pearson's correlation coefficient in G and H; the regression lines are shown with the 95% confidence interval (dotted lines).

current study, based on glucose status. Since spatial memory deficits and impaired glucose metabolism develop solely in H-Gluc mice, the phenotype of these mice can be thought of as susceptible, whereas mice that retain Int-Gluc levels appear resilient. Importantly, lowering the glucose levels of CSD-exposed animals by means of the SGLT2 inhibitor EMPA was beneficial for mice that were previously identified as H-Gluc but was detrimental for the mice that initially retained glucose levels within a normal range despite CSD. The poor spatial memory of the latter group probably results from glucose levels that, due to EMPA, fell below the normal range, analogous to the impaired spatial memory found in EMPA-treated control mice identified as L-Gluc (<125 mg/mL). Thus, our findings are congruent with glucose function having a commanding role in cognitive integrity so that both hyper- and hypoglycemia are linked to impaired spatial memory performance in the Y-maze. We cannot determine whether stress-induced hyperglycemia predicts spatial memory performance, as cognitive impairments may already have been affected during chronic stress (19). In any case, peripheral blood glucose levels 2 d post-CSD comprise valuable biomarkers, as these were instrumental in determining the effectiveness of EMPA treatment. Of note, the typical segregation into stress susceptibility or resilience is based on social avoidance of an unknown aggressor by CSD-exposed mice 1 d after the conclusion of the chronic stress (23, 28). Although we observed social avoidance by stressed mice, this behavior did not correlate with peripheral blood glucose levels 2 d following CSD (*SI Appendix*, Fig. S5).

The hyperphagia, glucose dysregulation, and memory deficits that emerged in CSD-exposed mice are features reminiscent of an emergent metabolic disorder, such as prediabetes DM2. Memory deficits appear as the most prominent cognitive deterioration in DM2 and are linked to hippocampal injury (29, 30). Cognitive impairments have an onset even before the development of DM2 (31). In line with these findings, the memory deficits found in our stressed mice also appeared early after CSD and were correlated positively with animals' hippocampal glucose levels. The DM2-associated cognitive deficits in humans have been suggested to relate to impaired hippocampal insulin function (32). Although insulin definitely plays an important role in memory formation (33), our findings suggest that CSD-induced hyperglycemia, in the absence of insulin resistance, is sufficient to cause memory deficits, corroborating the spatial memory impairments reported in a prediabetic rat model (34). A reduction of glucose concentrations, achieved by the recently approved antidiabetic EMPA, was beneficial to CSD-exposed mice that developed hyperglycemia. EMPA has been shown previously to exert beneficial effects in animal models of obesity and DM2 (35–37). Importantly, however, CSD did not induce a full-blown metabolic syndrome (e.g., DM2): Insulin and leptin levels remained unaltered, insulin resistance was absent, body weights were not affected, and the blood glucose-and HbA1c levels, although elevated, were not in a range typically associated with diabetes (26, 35). Instead, we propose that the stress-associated glucose dysfunction and memory deficits we observed in a subset of CSD-exposed mice could be considered a prodromal phase where additional environmental risk factors, such as poor dietary choices, might culminate in the full-blown disorder. Therefore, our identification of stress-susceptible individuals through glucose stratification allows early interventions to halt disease progression to prediabetes and beyond.

A key component of the stress response is the mobilization of energy stores, enabling the organism to dedicate energy toward processes involved in fight or flight (38). Throughout our CSD, all animals were defeated and attempted to flee from their opponent. As expected, social defeat induces a robust increase in circulating glucocorticoids in the peripheral blood (39), a phenomenon that can rapidly increase glucose levels in the bloodstream (12).

In agreement with these findings, we observed increased concentrations of both corticosterone and glucose 2 d post-CSD (day 12). However, these observations were not intercorrelated (*SI Appendix*, Fig. S1A). Moreover, glucose levels were not enhanced during CSD itself, and 1 wk following CSD, when glucose levels are markedly increased, corticosterone levels did not differ between controls and stressed mice. Thus, it appears that the CSD-induced hyperglycemia is not directly coupled to enhanced glucocorticoid levels. One possibility is that increased concentrations of glucocorticoids in the stressed mice lead to hyperphagia that in turn causes glucose levels to increase. Of note, glucocorticoids are known to stimulate food intake (40, 41), and, in line with the current findings, social stress in mice was found to induce hyperphagia (42). Although speculative, we thus imagine that glucose production during CSD is increased in part through hyperphagia but that hyperglycemia does not develop at this stage because glucose consumption may meet the energetic demands of stress. Our findings further suggest that post-CSD hyperphagia is more relevant for the progression of hyperglycemia than the hyperphagia that takes place during CSD, as caloric restriction imposed throughout the CSD did not prevent the development of post-CSD hyperglycemia, nor did it improve spatial memory. Therefore hyperphagia during CSD may represent a coping strategy of the animals under stress and can be regarded as allostatic load (43). As these severe energetic requirements during CSD have likely dropped considerably thereafter, we surmise that the hyperphagia that continues to take place post-CSD is maladaptive and is crucial in the development of peripheral and central hyperglycemia and spatial memory dysfunction.

Of equal importance to its production is the status of glucose uptake and breakdown. Results from the GTTs revealed that stressed mice exhibited attenuated peripheral glucose breakdown. Additionally, the reduced ^{18}F-FDG signals obtained by cerebral PET scans indicate that impaired cerebral glucose uptake is likely involved in the stress-related pathology. Since the brains of CSD-exposed mice were hyperglycemic, the diminished ^{18}F-FDG uptake can be explained by its competition with endogenous glucose for the available glucose-uptake sites. Compatible with this concept is the finding that acute glucose loading in healthy humans reduced cerebral ^{18}F-FDG uptake (44). Nevertheless, glucose levels in CSD-exposed mice are lastingly elevated, and functional adjustments at the level of glucose-uptake sites remain an additional possibility. GluTs are the main determinants of cellular glucose entry; the most prominent ones in the brain include GluT1 and GluT3; GluT4 expression is more restricted but involves the hippocampal area. We found a specific reduction in GluT1 protein expression on the cellular membrane in the brains of stressed animals but no changes in GluT3 and GluT4 expression levels. Congruent with our findings, in vitro studies showed that GluT1, but not GluT4, is glucose-regulated so that high glucose levels decrease its expression (45). Glucocorticoids have been shown to down-regulate GluT3 in the hypothalamus but did not affect hippocampal GluT3 expression (46, 47), which is also consistent with the unaltered hippocampal GluT3 levels we found in CSD-exposed mice.

CSD resulted in hyperglycemia and reduced ^{18}F-FDG uptake throughout the entire brain. Therefore it is not entirely clear why, during this hyperglycemic period, certain properties (novel object memory, anxiety-like behavior) remained unaltered but others (spatial memory in the Y-maze and the object location task as well as behavior in the forced swim test) were impaired. Importantly, both spatial memory and forced swim test performance are sensitive to hippocampal function (48, 49). For now, we speculate that the particular glucocorticoid receptor-related vulnerability of the hippocampus to stress (50, 51) is responsible for the selective stress-induced behavioral phenotype we

observed. However, we assessed mice on a limited number of behavioral tests and expect that CSD-induced functional consequences cover more than hippocampal impairments alone. For example, given the impact of stress on dopamine release in the nucleus accumbens and the ramifications for motivational aspects (52), CSD-induced disturbances are anticipated to involve accumbal function as well.

How elevated glucose concentrations in stress-susceptible mice can impair brain functions and lead to impaired spatial memory remain to be investigated. Intriguingly, CSD-mediated effects on food intake, physical activity, and the actions of glucocorticoids are routes through which neurogenesis may be affected in the stressed brain (53). For example, Lagace et al. (54) showed that at 4 wk after CSD mice that displayed social avoidance (i.e., the susceptible animals) had increased numbers of surviving neurons in the dentate gyrus. Largely in line with these findings, Kirshenbaum et al. (55) found that following CSD adult mice with reduced adolescent (but not adult) neurogenesis showed a resilient phenotype. However, in contrast to previous findings (54, 55), a very recent study (56) revealed that increasing neurogenesis actually confers resilience to chronic stress by inhibiting the activity of mature granule cells in the dentate gyrus. Regardless of the direction of effects, the long-term stress-induced functional changes observed in the current study could have been mediated, at least in part, through altered neurogenesis and or neuronal maturation. Apart from CSD effects on neurogenesis, underlying mechanisms may also include neurotransmitter synthesis, metabolic support for glial regulation of glutamate, or glucose-mediated neuroinflammation (57, 58). An altered NADH/NAD$^+$ balance may be seen as an early sign of glucose-related perturbations, and the presence of TBARS in the sample would indicate oxidative damage of lipids (58, 59). However, our results suggest that the effects of CSD-induced hyperglycemia are unlikely to involve modifications at the level of NAD$^+$/NADH or TBARS.

In conclusion, we demonstrated that CSD impairs spatial memory and affects peripheral as well as central glucose levels and glucose metabolism. These impairments can be treated post-CSD with EMPA when given to animals that develop hyperglycemia early after CSD but not when given to those that retained glucose levels within a normal range. Since both hyperglycemia (>150 mg/mL) and hypoglycemia (<125 mg/mL) were associated with spatial memory deficits, our findings suggest that glucose fluctuations should be kept within a relatively narrow range to preserve proper function and imply the existence of an inverted U-shaped curve, which is frequently invoked to explain the biphasic effects of glucocorticoids on cognition (60). We propose CSD and its classification based on individual glucose levels early poststress as a valuable tool to investigate social stress in the context of metabolic disturbances and associated mental dysfunction. The functional connection made in this study, namely between stress-related cognitive impairments and the emergence of metabolic dysfunction, may explain the high comorbidity found for diabetes and depression (61–63). Hence, our study further bridges the gap between stress-related pathologies and metabolic disorders and emphasizes the need for more interdisciplinary research with the ultimate goal of designing tailored treatment strategies.

Materials and Methods

Animals. Male C57BL/6J mice (Janvier) arrived at 8 wk of age in our animal facility (temperature = 22 ± 2 °C, relative humidity = 50 ± 5%). Mice were single-housed with food/water ad libitum in a light–dark cycle with lights on at 07:00 and off at 19:00 and were allowed to habituate for at least 1 wk before the onset of experiments. Retired male CD-1 mice breeders (Janvier) at least 12 wk of age upon arrival were used as aggressors in the CSD paradigm. Before behavioral experiments we tested the CD-1 mice to ensure aggressive behaviors would commence within a 1-min period (64) in a social

encounter with a C57BL/6J mouse. Our study involved only male mice, as the CD-1 mice used as the aggressors in the CSD paradigm do not typically attack female mouse intruders. Of note, application of male odorants to female intruders (65) or exposing the female intruder mice to lactating dams (66) may overcome these natural barriers. However, in the current study we focused on studying the role of stress-induced effects on glucose metabolism and avoided the inclusion of these confounding factors. Procedures concerning the insulin-tolerance test, hippocampal measurements of TBARS and NAD$^+$/NADH, and caloric restrictions are detailed in *SI Appendix*. All behavioral experiments were conducted between 09:00 and 14:00 by experimenters blind to treatment groups and were performed in accordance with the European directive 2010/63/EU for animal experiments and were approved by the local authorities (Animal Protection Committee of the State Government, Landesuntersuchungsamt Rheinland-Pfalz, Koblenz, Germany). The videos of all behavioral tests were scored manually by an experimenter blinded to the animals' treatment using The Observer XT12 software (Noldus Information Technology). Between testing, setups were cleaned with a 5% EtOH solution and dried with tissues. Behavioral testing occurred in custom-made sound-attenuating boxes under fixed-light conditions (37 lx). Detailed descriptions of the behavioral tests performed are provided in *SI Appendix*.

CSD. The CSD paradigm is a modification of published protocols (39, 64). C57 mice either were exposed to CSD or were kept as controls. CSD consisted of a social defeat in the home cage of the aggressor mouse (CD-1) lasting 10 s of aggressive encounter; these episodes were repeated three times with different aggressors and were separated by ~15-min interepisode intervals. During these intervals a metal grid was placed between the defeated animal (C57) and its aggressor, thereby temporarily removing the somatosensory component of the interaction. Following the triple social defeat, C57 mice were housed overnight with their opponent separated by the metal grid. The social defeat was repeated for 10 consecutive days. Control mice were placed in a novel cage for 90 s over 10 consecutive days, and their cages were also equipped with a metal grid to mimic the conditions experienced by the defeated mice. After CSD (or control conditions), mice were single-housed in a novel cage before further experimentation. No animals required exclusion for excessive wounding.

Peripheral Glucose Measurements. Animals were fasted for 1 h before peripheral blood glucose measurements to exclude variability caused by recent food intake. Peripheral blood was obtained by tail-cut under unrestrained and stress-free conditions (67); the first drop of blood was always discarded. Morning blood glucose was measured using an electronic handheld glucometer (Accu-Chek; Roche). Three consecutive measurements of blood glucose were taken and averaged to establish reliable values. For urine glucose measurements, 7 d after CSD and 5 d after EMPA or vehicle treatment in the diet, the animas was placed in an open field without food and water and was returned to its home-cage after it had urinated. The urine was collected with a syringe and frozen at −20 °C until processing. Urine was diluted 4,000× and analyzed using a Glucose Colorimetric Assay Kit (catalog no. K606-100; BioVision).

Peripheral Measurements of HbA1c. HbA1c levels were measured from whole blood by the Mouse Hemoglobin A1c (HbA1c) Kit (catalog no. 80310; Crystal Chem, Inc.) according to the manufacturer's instructions. Whole blood was obtained by tail-cut under unrestrained conditions, collected in EDTA tubes, and stored at −20 °C until processing.

Peripheral Corticosterone, Insulin, and Leptin Measurements. Levels of morning circulating corticosterone, insulin, or leptin in blood plasma were measured by the Corticosterone ELISA Kit (catalog no. ADI-900-0979; Enzo Life Sciences), the Ultra Sensitive Mouse Insulin ELISA Kit (catalog no. 90080; Crystal Chem, Inc.), or the Mouse Leptin ELISA Kit (catalog no. 90030; Crystal Chem, Inc.), respectively, according to the manufacturers' instructions. Blood was obtained by tail-cut under unrestrained conditions, collected in EDTA tubes, and spun in a precooled centrifuge at 10,000 × g for 10 min at 4 °C, after which the plasma was extracted and frozen at −80 °C until processing. The plasma for leptin measurement was diluted 10×.

Dissection of Adrenal Glands. Mice were decapitated, and the skin overlying the abdomen was cut. The adrenals were carefully removed from the surrounding fat tissue using forceps and microscissors.

GTT. The GTT was performed as recommended in the literature (68). Animals were subjected to food deprivation for 15 h before glucose measurement.

Peripheral blood glucose or insulin measurements were taken at baseline and at 30-min intervals for 2 h following i.p. injection of a glucose bolus (2 g/kg).

Central Glucose imBI. Mice were killed by cervical dislocation, and the whole body was submerged in liquid nitrogen within 10 s to preserve native glucose concentrations. The frozen corpse was secured in a vice, and the head was separated from the body with an electric handheld drill equipped with a diamond cutting disk [diameter (∅) 38 × 0.6 mm; Proxxon GmbH]. The brain was manually dissected from the skull with a handheld saw while the tissue was kept frozen on dry ice. The metabolic distributions of glucose were measured in cryosections of the snap-frozen samples using the imBI method as previously described (69–72). In brief, tissue cryosections were brought into contact with a reaction solution, coupling the enzymatic conversion of glucose to the light emission of a luciferase system. The light emission was detected using a light-sensitive CCD camera system (iXonEM + DU-888; Andor Technology PLC), resulting in 2D intensity maps. The intensity maps were calibrated to local metabolite concentration (μmol/g tissue) in viable tissue areas using appropriate standards and a parallel H&E-stained cryosection for association of the metabolite distribution with tissue structure.

Stereotaxic Surgery for Hippocampal Cannulation and Glucose Infusion. Mice were anesthetized in an isoflurane-filled box (Forene; AbbVie) and secured in a Stoelting stereotaxic frame under gas anesthesia [2% isoflurane in O_2 (4 L/min)]. Anesthesia was confirmed by pinching the hind-paw. Analgesia was achieved with an injection of meloxicam (Metacam, 0.5 mg/kg i.m.; Boehringer-Ingelheim) and by putting Metacam in the drinking water for 1 wk (1/1,000 vol/vol). The eyes were covered with Bepanthen (Bayer) to avoid dehydration, and the skin on top of the skull was shaved and disinfected using Braunol (Braun), after which the skin was exposed through a longitudinal cut. The membrane lining the skull was removed, the skull surface was roughened using a scalpel, and a drop of 30% H_2O_2 was applied. Four small holes were drilled, two for the placement of stainless steel cannulae (Plastics One) aimed at the dorsal hippocampus according to stereotaxic coordinates [anteroposterior, −2.5 mm from bregma; dorsoventral, −0.8 mm from the skull surface; and mediolateral, ±2.5 mm from bregma (73)], and two for the introduction of anchoring screws. Dental acrylic cement (DuraLay; Reliance) was applied to fix the cannula, and stitches were made to close the wound. An analgesic spray (Lidocaine; AstraZeneca) was applied to the suture. Animals were allowed to recover for 2 wk, after which we handled animals for 3 min/d for three consecutive days. The following day, we performed the cognitive Y-maze (*SI Appendix, Cognitive Y-Maze*) to assess spatial memory. Immediately after the habituation phase of the Y-maze, we inserted injectors extending 1 mm from the tip of the cannulae, and mice were infused (0.5 μL bilateral, at an infusion speed of 0.2 μL/min; an additional minute postinfusion was included to allow spread of the infusate) with either a glucose solution (2.7 μg glucose per hippocampus) or vehicle (0.9% NaCl). The concentration of infused glucose solution was calculated based on the average hippocampal glucose concentrations we observed for CSD-exposed mice using imBI (1.5 μmol/g) (Fig. 3 C and D), the molecular weight of glucose (180 g/mol), and the expectation that the infusions would reach about 10 mg of hippocampal tissue per side. Directly after the glucose infusion, the animals were returned to the home cage for the remainder of the intertrial interval before the test phase of the Y-maze began. We verified correct targeting of the cannulae by ink injection [bilateral infusion of 0.5 μL of Evans blue (0.1%)] postmortem (Fig. 3H).

¹⁸F-FDG PET Scanning. All animals fasted ~1 h before PET acquisition. The mice were placed head-down prone and were anesthetized by 2% isoflurane vaporized in 70% O_2 delivered through a nose cone. A Focus 120 microPET scanner (Siemens/CTI) was used for data collection. The system has lutetium oxyorthosilicate detectors for coincidence detection (timing window: 6 ns) with a size of $1.5 × 1.5 × 1.0$ mm³. The resolution at the center of the field of view is ≤1.4 mm. The PET tracer ¹⁸F-FDG (PET Net GmbH) was injected i.p. Emission scans in list mode data format were acquired for 15 min at 45 min postinjection. PET list mode data were reconstructed using filtered back-projection (ramp filter, cutoff = 0.5) into 95 slices of 0.80-mm thickness (pixel size: $0.87 × 0.87$ mm²) and a matrix of $128 × 128$ pixels. Corrections were applied for dead time, randoms, and radioactive decay. The PET image was coregistered to an MR T2 mouse template (74) as provided by PMOD software v. 3.4 (PMOD Technologies LLC). Seven brain regions were selected from the PMOD brain volume-of-interest template and were projected onto the PET images: cortex cerebri (81 mm³), striatum (13 mm³), thalamus (43 mm³), dorsal hippocampus (11 mm³), hypothalamus (9 mm³), amygdala (6 mm³), and the cerebellar cortex (35 mm³) from the whole brain (222 mm³). ¹⁸F-FDG uptake was expressed as normalized radioactivity = measured radioactivity in the PET image (kBq/mL)/injected radioactivity (kBq) in units of [%ID/mL]. As we expected to find effects in the dorsal part of the hippocampus, normalized radioactivity values of this brain region were compared using a two-sided Student's independent-samples t test (SPSS 23; IBM). In further exploratory analyses Student's independent-samples t tests were calculated for the remaining volumes of interest.

Western Blot. Dorsal hippocampi were dissected and quickly frozen on dry ice. Brain tissue was then processed to purify the cytosol and the membrane fractions using the ProteoExtract Subcellular Proteome Extraction Kit (539790; Calbiochem) according to the manufacturer's instructions. Equal amounts of proteins were denatured for 5 min at 60 °C, separated by 10% SDS/PAGE, and transferred onto nitrocellulose membranes as previously described (75). The membranes were incubated with the following primary antibodies: rabbit anti-GluT1 (1:2,000; 07-1401; Millipore); rabbit anti-GluT3 (1:2,000; ab191071; Abcam); and mouse anti-GluT4 (1:2,000; 2213; Cell Signaling), followed by incubation with the appropriate HRP-conjugated secondary antibodies (Dianova) and ECL detection (Westar; Cyanagen). Chemiluminescence was visualized and quantified with the Fusion SL system (Vilber Lourmat Peqlab), and band intensities were normalized to β-tubulin III (1:2,000; T8660; Sigma-Aldrich).

EMPA Administration. Mice received a custom-made diet containing 0.03% EMPA (Jardiance; Adipogen Life Sciences) or a control diet (vehicle) (ssniff Spezialdiäten GmbH) commencing 2 d post-CSD.

Statistical Analyses. All samples represent biological replicates. Sample sizes are indicated in the figure legends. Values are expressed as mean ± SEM. Unpaired two-tailed Student's t tests were used to compare sets of data obtained from two independent groups of animals, using a one-sample t test against chance level and one- or two-way ANOVA followed by Bonferroni post hoc tests when appropriate. Pearson's correlation coefficient was used to measure linear correlation between two sets of data. P values are reported in figure legends, with $P < 0.05$ considered statistically significant. All data were analyzed using Prism version 6 (GraphPad Software, Inc.).

1. Erbsloh F, Bernsmeier A, Hillesheim H (1958) [The glucose consumption of the brain & its dependence on the liver]. *Arch Psychiatr Nervenkr Z Gesamte Neurol Psychiatr* 196: 611–626. German.
2. Picard M, McEwen BS, Epel ES, Sandi C (2018) An energetic view of stress: Focus on mitochondria. *Front Neuroendocrinol* 49:72–85.
3. Hackett RA, Steptoe A (2017) Type 2 diabetes mellitus and psychological stress–A modifiable risk factor. *Nat Rev Endocrinol* 13:547–560.
4. Bryan RM, Jr (1990) Cerebral blood flow and energy metabolism during stress. *Am J Physiol* 259:H269–H280.
5. Osborne DM, Pearson-Leary J, McNay EC (2015) The neuroenergetics of stress hormones in the hippocampus and implications for memory. *Front Neurosci* 9:164.
6. Dimsdale JE (2008) Psychological stress and cardiovascular disease. *J Am Coll Cardiol* 51:1237–1246.
7. Kelly SJ, Ismail M (2015) Stress and type 2 diabetes: A review of how stress contributes to the development of type 2 diabetes. *Annu Rev Public Health* 36: 441–462.
8. Steptoe A, Kivimäki M (2013) Stress and cardiovascular disease: An update on current knowledge. *Annu Rev Public Health* 34:337–354.
9. Zhuang QS, Shen L, Ji HF (2017) Quantitative assessment of the bidirectional relationships between diabetes and depression. *Oncotarget* 8:23389–23400.
10. Mergenthaler P, Lindauer U, Dienel GA, Meisel A (2013) Sugar for the brain: The role of glucose in physiological and pathological brain function. *Trends Neurosci* 36: 587–597.
11. Kopschina Feltes P, et al. (2017) Repeated social defeat induces transient glial activation and brain hypometabolism: A positron emission tomography imaging study. *J Cereb Blood Flow Metab*, 271678X17747189.
12. Picard M, Juster RP, McEwen BS (2014) Mitochondrial allostatic load puts the 'gluc' back in glucocorticoids. *Nat Rev Endocrinol* 10:303–310.
13. Morava E, Kozicz T (2013) Mitochondria and the economy of stress (mal)adaptation. *Neurosci Biobehav Rev* 37:668–680.
14. Videbech P (2000) PET measurements of brain glucose metabolism and blood flow in major depressive disorder: A critical review. *Acta Psychiatr Scand* 101:11–20.

NEUROSCIENCE

15. Roberts RO, et al. (2014) Diabetes and elevated hemoglobin A1c levels are associated with brain hypometabolism but not amyloid accumulation. *J Nucl Med* 55:759–764.
16. Biessels GJ, Reagan LP (2015) Hippocampal insulin resistance and cognitive dysfunction. *Nat Rev Neurosci* 16:660–671.
17. Watson K, Nasca C, Aasly L, McEwen B, Rasgon N (2018) Insulin resistance, an unmasked culprit in depressive disorders: Promises for interventions. *Neuropharmacology* 136:327–334.
18. McEwen BS (2003) Mood disorders and allostatic load. *Biol Psychiatry* 54:200–207.
19. Conrad CD (2010) A critical review of chronic stress effects on spatial learning and memory. *Prog Neuropsychopharmacol Biol Psychiatry* 34:742–755.
20. Sousa N, Lukoyanov NV, Madeira MD, Almeida OF, Paula-Barbosa MM (2000) Reorganization of the morphology of hippocampal neurites and synapses after stress-induced damage correlates with behavioral improvement. *Neuroscience* 97:253–266.
21. van der Kooij MA, et al. (2014) Role for MMP-9 in stress-induced downregulation of nectin-3 in hippocampal CA1 and associated behavioural alterations. *Nat Commun* 5:4995.
22. O'Keefe J, Nadel L (1978) *The Hippocampus as a Cognitive Map* (Oxford Univ Press, Oxford, UK).
23. Krishnan V, et al. (2007) Molecular adaptations underlying susceptibility and resistance to social defeat in brain reward regions. *Cell* 131:391–404.
24. Simpson IA, Carruthers A, Vannucci SJ (2007) Supply and demand in cerebral energy metabolism: The role of nutrient transporters. *J Cereb Blood Flow Metab* 27:1766–1791.
25. Juster RP, McEwen BS, Lupien SJ (2010) Allostatic load biomarkers of chronic stress and impact on health and cognition. *Neurosci Biobehav Rev* 35:2–16.
26. Gallo LA, et al. (2016) Once daily administration of the SGLT2 inhibitor, empagliflozin, attenuates markers of renal fibrosis without improving albuminuria in diabetic db/db mice. *Sci Rep* 6:26428.
27. Der-Avakian A, Mazei-Robison MS, Kesby JP, Nestler EJ, Markou A (2014) Enduring deficits in brain reward function after chronic social defeat in rats: Susceptibility, resilience, and antidepressant response. *Biol Psychiatry* 76:542–549.
28. Anacker C, et al. (2016) Neuroanatomic differences associated with stress susceptibility and resilience. *Biol Psychiatry* 79:840–849.
29. Gold SM, et al. (2007) Hippocampal damage and memory impairments as possible early brain complications of type 2 diabetes. *Diabetologia* 50:711–719.
30. Strachan MW, Deary IJ, Ewing FM, Frier BM (1997) Is type II diabetes associated with an increased risk of cognitive dysfunction? A critical review of published studies. *Diabetes Care* 20:438–445.
31. van Bussel FC, et al. (2016) Functional brain networks are altered in type 2 diabetes and prediabetes: Signs for compensation of cognitive decrements? The Maastricht study. *Diabetes* 65:2404–2413.
32. McNay EC, Recknagel AK (2011) Brain insulin signaling: A key component of cognitive processes and a potential basis for cognitive impairment in type 2 diabetes. *Neurobiol Learn Mem* 96:432–442.
33. van der Heide LP, Ramakers GM, Smidt MP (2006) Insulin signaling in the central nervous system: Learning to survive. *Prog Neurobiol* 79:205–221.
34. Soares E, et al. (2013) Spatial memory impairments in a prediabetic rat model. *Neuroscience* 250:565–577.
35. Lin B, et al. (2014) Glycemic control with empagliflozin, a novel selective SGLT2 inhibitor, ameliorates cardiovascular injury and cognitive dysfunction in obese and type 2 diabetic mice. *Cardiovasc Diabetol* 13:148.
36. Vallon V, et al. (2014) SGLT2 inhibitor empagliflozin reduces renal growth and albuminuria in proportion to hyperglycemia and prevents glomerular hyperfiltration in diabetic Akita mice. *Am J Physiol Renal Physiol* 306:F194–F204.
37. Kern M, et al. (2016) The SGLT2 inhibitor empagliflozin improves insulin sensitivity in db/db mice both as monotherapy and in combination with linagliptin. *Metabolism* 65:114–123.
38. Munck A, Guyre PM, Holbrook NJ (1984) Physiological functions of glucocorticoids in stress and their relation to pharmacological actions. *Endocr Rev* 5:25–44.
39. Jene T, et al. (2018) Temporal profiling of an acute stress-induced behavioral phenotype in mice and role of hippocampal DRR1. *Psychoneuroendocrinology* 91:149–158.
40. Green PK, Wilkinson CW, Woods SC (1992) Intraventricular corticosterone increases the rate of body weight gain in underweight adrenalectomized rats. *Endocrinology* 130:269–275.
41. Zakrzewska KE, et al. (1999) Induction of obesity and hyperleptinemia by central glucocorticoid infusion in the rat. *Diabetes* 48:365–370.
42. Sanghez V, et al. (2013) Psychosocial stress induces hyperphagia and exacerbates diet-induced insulin resistance and the manifestations of the Metabolic syndrome. *Psychoneuroendocrinology* 38:2933–2942.
43. McEwen BS, et al. (2015) Mechanisms of stress in the brain. *Nat Neurosci* 18:1353–1363.
44. Ishibashi K, Wagatsuma K, Ishiwata K, Ishii K (2016) Alteration of the regional cerebral glucose metabolism in healthy subjects by glucose loading. *Hum Brain Mapp* 37:2823–2832.
45. Wertheimer E, Sasson S, Cerasi E, Ben-Neriah Y (1991) The ubiquitous glucose transporter GLUT-1 belongs to the glucose-regulated protein family of stress-inducible proteins. *Proc Natl Acad Sci USA* 88:2525–2529.
46. Cherian AK, Briski KP (2010) Effects of adrenalectomy on neuronal substrate fuel transporter and energy transducer gene expression in hypothalamic and hindbrain metabolic monitoring sites. *Neuroendocrinology* 91:56–63.
47. Reagan LP, et al. (1999) Regulation of GLUT-3 glucose transporter in the hippocampus of diabetic rats subjected to stress. *Am J Physiol* 276:E879–E886.
48. Shirayama Y, Chen AC, Nakagawa S, Russell DS, Duman RS (2002) Brain-derived neurotrophic factor produces antidepressant effects in behavioral models of depression. *J Neurosci* 22:3251–3261.
49. Deltheil T, et al. (2008) Behavioral and serotonergic consequences of decreasing or increasing hippocampus brain-derived neurotrophic factor protein levels in mice. *Neuropharmacology* 55:1006–1014.
50. McEwen BS (2001) Plasticity of the hippocampus: Adaptation to chronic stress and allostatic load. *Ann N Y Acad Sci* 933:265–277.
51. Conrad CD (2008) Chronic stress-induced hippocampal vulnerability: The glucocorticoid vulnerability hypothesis. *Rev Neurosci* 19:395–411.
52. Lemos JC, et al. (2012) Severe stress switches CRF action in the nucleus accumbens from appetitive to aversive. *Nature* 490:402–406.
53. van Praag H, Fleshner M, Schwartz MW, Mattson MP (2014) Exercise, energy intake, glucose homeostasis, and the brain. *J Neurosci* 34:15139–15149.
54. Lagace DC, et al. (2010) Adult hippocampal neurogenesis is functionally important for stress-induced social avoidance. *Proc Natl Acad Sci USA* 107:4436–4441.
55. Kirshenbaum GS, Lieberman SR, Briner TJ, Leonardo ED, Dranovsky A (2014) Adolescent but not adult-born neurons are critical for susceptibility to chronic social defeat. *Front Behav Neurosci* 8:289.
56. Anacker C, et al. (2018) Hippocampal neurogenesis confers stress resilience by inhibiting the ventral dentate gyrus. *Nature* 559:98–102.
57. McNay EC, Gold PE (2002) Food for thought: Fluctuations in brain extracellular glucose provide insight into the mechanisms of memory modulation. *Behav Cogn Neurosci Rev* 1:264–280.
58. Yan LJ (2014) Pathogenesis of chronic hyperglycemia: From reductive stress to oxidative stress. *J Diabetes Res* 2014:137919.
59. Teodoro JS, Rolo AP, Palmeira CM (2013) The NAD ratio redox paradox: Why does too much reductive power cause oxidative stress? *Toxicol Mech Methods* 23:297–302.
60. de Kloet ER, Oitzl MS, Joëls M (1999) Stress and cognition: Are corticosteroids good or bad guys? *Trends Neurosci* 22:422–426.
61. Chen S, et al. (2016) Association of depression with pre-diabetes, undiagnosed diabetes, and previously diagnosed diabetes: A meta-analysis. *Endocrine* 53:35–46.
62. Roy T, Lloyd CE (2012) Epidemiology of depression and diabetes: A systematic review. *J Affect Disord* 142(Suppl):S8–S21.
63. Moulton CD, Pickup JC, Ismail K (2015) The link between depression and diabetes: The search for shared mechanisms. *Lancet Diabetes Endocrinol* 3:461–471.
64. Golden SA, Covington HE, 3rd, Berton O, Russo SJ (2011) A standardized protocol for repeated social defeat stress in mice. *Nat Protoc* 6:1183–1191.
65. Harris AZ, et al. (2018) A novel method for chronic social defeat stress in female mice. *Neuropsychopharmacology* 43:1276–1283.
66. Jacobson-Pick S, Audet MC, McQuaid RJ, Kalvapalle R, Anisman H (2013) Social agonistic distress in male and female mice: Changes of behavior and brain monoamine functioning in relation to acute and chronic challenges. *PLoS One* 8:e60133.
67. Fluttert M, Dalm S, Oitzl MS (2000) A refined method for sequential blood sampling by tail incision in rats. *Lab Anim* 34:372–378.
68. Ayala JE, et al.; NIH Mouse Metabolic Phenotyping Center Consortium (2010) Standard operating procedures for describing and performing metabolic tests of glucose homeostasis in mice. *Dis Model Mech* 3:525–534.
69. Sattler UG, et al. (2010) Glycolytic metabolism and tumour response to fractionated irradiation. *Radiother Oncol* 94:102–109.
70. Mueller-Klieser W, Walenta S (1993) Geographical mapping of metabolites in biological tissue with quantitative bioluminescence and single photon imaging. *Histochem J* 25:407–420.
71. Walenta S, Schroeder T, Mueller-Klieser W (2004) Lactate in solid malignant tumors: Potential basis of a metabolic classification in clinical oncology. *Curr Med Chem* 11:2195–2204.
72. Walenta S, Voelxen NF, Sattler UG, Mueller-Klieser W (2014) Localizing and quantifying metabolites in situ with luminometry: Induced metabolic bioluminescence imaging (imBI). *Neuromethods* 90:195–216.
73. Paxinos G, Franklin K (2012) *Paxinos and Franklin's the Mouse Brain in Stereotaxic Coordinates* (Academic, San Diego), 4th Ed.
74. Mirrione MM, et al. (2007) A novel approach for imaging brain-behavior relationships in mice reveals unexpected metabolic patterns during seizures in the absence of tissue plasminogen activator. *Neuroimage* 38:34–42.
75. Ruehle S, et al. (2013) Cannabinoid CB1 receptor in dorsal telencephalic glutamatergic neurons: Distinctive sufficiency for hippocampus-dependent and amygdala-dependent synaptic and behavioral functions. *J Neurosci* 33:10264–10277.